



Wave Hindcasting and Anchoring Activities in Ancient Harbours: The Impact of Coastal Dynamics on Ancient Carthago Nova (Cartagena, Spain)

Felipe Cerezo-Andreo¹ · Francisco J. López-Castejón² · Sebastian F. Ramallo-Asensio³ · Javier Gilabert-Cervera²

© Springer Science+Business Media, LLC, part of Springer Nature 2020

Abstract

This study analyses nautical harbour activities and their spatial distribution using a high-resolution method of wind-wave hindcasting, in order to identify the location of safe and sheltered anchorage areas. We apply this methodological approach to evaluate the ancient harbour of Carthago Nova from the Punic period to the Late Roman period (third century BC–fourth century AD). Literary sources have defined Carthago Nova (Cartagena, Spain) as the only natural harbour of *Hispania* and one of the best in the Mediterranean, with Escombreras Island as the main natural feature that protects the harbour. Due to the scarcity of archaeological evidence and the transformation the harbour has undergone over time, this study has been considered necessary and carried out in order to supersede the current general and anachronistic observations of wind-wave effects. Through an interdisciplinary approach, we analyse one of the main factors that determines the safe anchorage of ships: coastal wind waves. The modelling and simulation of waves have been applied using the SWAN model, paleo-topographic reconstruction, and maritime archaeological data. By means of GIS spatial analysis, an Anchorage Safety Index has been established that computes data from paleo-bathymetry, wind, and simulated wave height. This high-resolution analysis allows us to assess in detail the impact of coastal and island topography on nautical activities inside ancient harbours.

Keywords Harbour archaeology · Wind-wave simulation · SWAN model · Ancient navigation · Hydrodynamic analysis

✉ Felipe Cerezo-Andreo
felipe.cerezo@uca.es

¹ Department of History, Geography and Archaeology, Maritime Archaeology Area, Faculty of Arts and Philosophy, University of Cádiz, Av. Dr. Gómez Ulla s/n, CP: 11003 Cádiz, Spain

² Department of Chemical and Environmental Engineering, Technical University of Cartagena, CP: 30203 Cartagena, Spain

³ Department of Prehistory and Archaeology, University of Murcia, CP: 30001 Murcia, Spain

Introduction

The study of ancient harbours using geoarchaeological technologies has been growing rapidly over recent years (Morhange et al. 2014; Stock et al. 2013). The synergy between these techniques and hydrodynamic modelling in harbour basins (Millet et al. 2000, 2014) and marine spaces (Safadi 2016) provides a powerful tool for maritime archaeology studies and for analysing site formation processes (Fernández-Montblanc et al. 2018). In order to identify the most likely locations of anchoring areas in the harbour space of ancient Carthago Nova (Cartagena, Spain), we combine geoarchaeological technologies, GIS analysis, and wind-wave modelling based on the findings from underwater archaeological data and identification of anchorage boundaries defined by the average rate of wave height. The model has been applied to three different time periods from the Punic foundations of the city (ca. 228 BC) to the Late Roman period (ca. AD 350). In this way, we can test the validity of the approach and its application for the study of other ancient harbours.

This research was carried out under the ARQUEOTOPOPOS Project, a research project that, since 2012, focuses on the evolution of the paleo-landscape of ancient Carthago Nova from a diachronic and interdisciplinary perspective (Fig. 1) (Ramallo Asensio et al. 2016). It is, however, also important to reference the results of other studies on the ancient harbour areas of Carthago Nova, especially for the Punic and Roman periods (third century BC–fourth century AD) (Cerezo-Andreo 2017; Manteca et al. 2017; Torres et al. 2018).

Ever since its foundation at the end of the third century BC, ancient Carthago Nova was one of the most important harbours in the western Mediterranean. Titus Livius (26. 43. 8.) describes it as “the one anchorage between the Pyrenees and Gades” and Polybius (10. 8. 2.) as “the only town in Iberia which possessed a harbour suitable for a fleet and naval force”. It

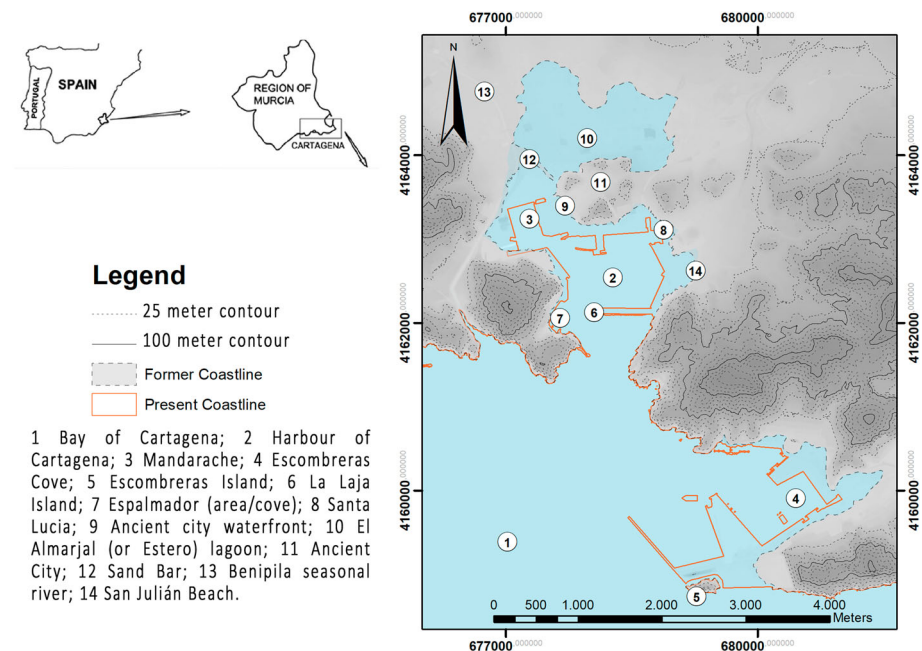


Fig. 1 Ancient Carthago Nova bay and harbour with the main topographical features cited in the text

was indeed a natural harbour in an estuarine area 2500 m long N–S and 1500 m wide E–W, surrounded by high mountains and with a small island (probably Escombereras Island) at the harbour entrance protecting it from waves (Ramallo Asensio and Martínez Andreu 2010). To the north there was a coastal lagoon (Fig. 1, #10), too shallow during the chronology of this study to have significant anchorage activities (Torres et al. 2018). Polybius, Titus Livius, and Strabo, as well as numerous mediaeval and modern authors, praise, amongst the many qualities and advantages of the city, the excellent conditions of its natural harbour: a wide deep bay, with calm waters and very well protected from the effect of the winds and waves.

According to Arnaud (2005), the nautical use of harbour spaces is determined, amongst other things, by the safety of the anchorage, which is mainly affected by wind waves, driven by frequent wind regimes and tempest or medicanes (Kaniewski et al. 2016). The small tidal amplitude in this area (about 20 cm)¹ and the absence of shallow navigation channels mean that daily tidal changes are not a factor to consider in our case. However, due to significant changes in the coastal morphology of harbour spaces, extrapolation of current data to evaluate the impact of wind waves on the ancient harbour activities is no longer possible.

The aim of this study is to address the following questions: (1) to what extent did the coastal topography and certain natural features, such as Escombereras Island, serve as determining factors in providing protection for safe anchorage in the harbour? (2) Where were the safest anchorage areas within the natural harbour of ancient Carthago Nova? (3) The purpose of a breakwater is to create an area of calm water between the open harbour space and the quays or *rippa* where the ships are moored. In ancient Carthago Nova, there are no archaeological remains of this kind of infrastructure but there is an inscription (*CIL* II 3434) that has been connected to the construction of a breakwater in *opus pilarum* (Abascal Palazón and Ramallo Asensio 1997: 71). It is possible to identify probable locations for ancient breakwaters by relating findings from underwater archaeological data to wind-wave hindcasting?

Methodology

To answer these questions, we present here the results of wind-wave hindcasting numerical simulations for three different topographic and paleo-bathymetric configurations—corresponding to three different time periods—with five wind scenarios each—each corresponding to higher occurrence winds. The first numerical simulation was performed over the reconstructed bathymetry during the city's Punic foundation (third century BC). The second simulation is during the first century BC (Late Roman Republican period) and, the third the Late Roman period (fourth century AD). The simulations shown here were selected as they represent the three most significant periods of harbour activity and maritime trade in ancient Carthago Nova. To check the validity and coherence of these results, two more simulations were carried out: one using very accurate cartography from the eighteenth century AD and another for current (present day) bathymetry (2017). These two extra simulations were run for the five dominant wind scenarios. However, the results of these last two simulations are not presented here, as they were only used as a check to test data validity and model outputs—which are beyond the scope of this present article. The bathymetry from the eighteenth century AD is shown in Fig. 6 only for comparison purposes.

In order to analyse a chronologically coherent coastline, we have used the results of a geoarchaeological study of ancient Carthago Nova, which enables us to offer a detailed recon-

¹ The tide measurement for this harbour has been obtained from the official repository of <http://www.puertos.es/es-es/oceanografia/Paginas/portus.aspx>, last accessed in December 2019.

struction of the coastline evolution, the topographic changes and the evolution of bathymetry and marine environments through more than 20 ¹⁴C derived dates (Manteca et al. 2017; Torres et al. 2018). Archaeological data were used to reconstruct the limits of the earlier harbour and the ancient port structures through GIS mapping. Archaeological finds and historical data are also essential to be able to identify anchorage areas, shipwreck sites, and port structures, including modern and contemporary modifications (dredging) of the entire harbour area.

After producing a GIS database, a climatological and oceanographical study of the area was done. Wind and wave regimes were scrutinized using a macro and micro scale analysis, as well as examination of the most common climatic conditions for long term anchoring activities, as well as other less common scenarios for evaluating storms or other high-energy events. With the results of these topographical and oceanographical data, a third-generation Simulating WAVes Nearshore—SWAN model (Delft University of Technology), was conducted on these three chronological simulations.

Once the different scenarios have been simulated, it was possible to analyse the harbour use from a nautical point of view. This approach has been addressed elsewhere (Millet et al. 2000, 2014), but we have tried to take it further by using GIS to create a dialogue between the archaeological data, which consists of finds from both terrestrial and anchorage contexts, and shipwreck sites, and by analysing nautical activities and the changing locations of anchoring spaces in the harbour. This kind of analysis helps to explain why in some cases, for example, an anchorage context can be located in an apparently dangerous area.

These results have permitted us to analyse the accessibility for ships and propose a new type of analysis: the Anchorage Safety Index (ASI). From a micro-topographic perspective, and by relating synoptic conditions (such as wave action on ships) and archaeological data, it is thus possible to identify the safest or most dangerous sections of the harbour for anchoring.

Historical Background and Previous Geoarchaeological Research

The Bay of Cartagena is located in a fault fracture between two large mountain ranges (that reach over 250 m above sea level in elevation), making it a well-sheltered space from N, E, W, SE, and SW local winds (Lillo Carpio and Rodríguez Estrella 1996; Seisdedos et al. 2013), with only its narrow entrance exposed to southern winds.

Despite the absence of clear ancient harbour structures, the findings from maritime landscape analysis and geoarchaeological and underwater archaeological studies (Cerezo-Andreo 2016) have made it possible to identify ancient anchoring contexts. Evidence from underwater archaeological investigations demonstrates changes in the maritime use of the harbour over time. These sites can be interpreted as anchorage areas, or as shipwreck sites, thus revealing the location of unsafe areas within the harbour limits (Pinedo Reyes 1996: 199).

The Harbour in Literary Sources

The natural protection of the harbour of Cartagena is characterised by high topography and indented coastline. The harbour (Fig. 1, #2) lies within the interior of the Bay of Cartagena (Fig. 1, #1), where there is a fracture in the high Baetica mountain system that gives access, through a narrow channel of 600 m width, to the harbour itself. The harbour is oval in plan, surrounded by mountains with elevations that exceed 250 m above sea level. To the north-west, a narrow channel, about 400 m wide, gives access to the estuarine harbour area known

as the Mandarache (Fig. 1, #3), which was the main mooring area from the third century BC to the mid-sixteenth century AD.

The harbour's qualities for providing shelter for vessels and the nautical conditions of the area have been described since Antiquity, and there are many written sources which provide examples of this. The earliest description is based on an archaic Massaliote Periplus, a sailing pilot possibly dating back to the sixth century BC and preserved in the fourth century AD by **Avienus**. In it are descriptions of sea routes used by sailors in their journeys around Europe. In *Or. Mar.* (v. 445–448), **Namnatius portus** is named and traditionally identified with the Bay of Cartagena (González Ponce 1995:174) and is described as a area which is well protected from the prevailing winds. Of even greater significance is the description of the city and its surroundings, given by **Polybius** (second century BC; Plb. 10.10) where he focuses on its peculiar topography, high mountain range, and its calm harbour. What is notable about this description is the role of an island, traditionally identified as Escomberas Island, which, according to **Strabo** (first century AD; Strab. 3.4.6) protects the mouth of the harbour from the frequent and dangerous waves coming from the south-east. This description of the bay as a large natural harbour of calm waters, girded by high mountains and protected by an island, is repeated in later sources such as **Titus Livius** (first century AD; 26.42.8) and **Appian** (second century AD; *Ib.* 20). **Virgil** (first century BC, *Aen.*, 1.569–69), relates the arrival of Aeneas on the coast of Africa and portrays an archetype of a natural harbour, a description in which several researchers have suggested is a re-creation of the topography of ancient Carthago Nova, although there is no conclusive evidence for this (Conde Guerri 2003: 59).

Carthago Nova became the topographical paradigm of a natural harbour in the maritime knowledge of Antiquity: a deep round bay, surrounded by mountains and with an island at its mouth that protected it from storms, thus maintaining calm inner waters. The continuity of these conditions can be traced to mediaeval and modern times, as we can see in Islamic texts from the twelfth century AD, such as that of Al-Qartayanni (Guillermo Martínez 2014:33), or eighteenth-century pilots (Tofiño de San Miguel 1787).

Archaeological Data

The archaeological data concerning the port area of ancient Carthago Nova can be ascertained from urban and underwater excavations. The analysis of this information has allowed for the identification of two types of contexts related to nautical activity that are affected by waves and winds: anchoring and wrecking (Fig. 2). On the one hand, this article will focus on the archaeological contexts of anchorages, enabling us to explore the problem of daily anchorage in a harbour, rather than on exceptional or anomalous situations. An anchorage context can be studied through diachronic archaeological data and, more importantly, allow for scrutiny of specific use of maritime space. Wrecks, on the other hand, will help us identify hazardous areas such as those where waves can push boats towards rocks, like in the eastern harbour basin sector. One should bear in mind that some wrecks may have happened not because of adverse weather conditions, but due to accidents which took place within the harbour area itself, such as a fire, collisions between vessels or even acts of war.

The **Mandarache** (Fig. 1, #3) stands out as the **main anchorage area**, in which more than three ancient shipwrecks and anchoring contexts can be identified. Also worthy of note is the anchorage located at the access point to the Mandarache, on the south-western **waterfront of the city** (Fig. 1, #9), where a wreck from the Severan period (third century AD) has been documented, in addition to an area of land with several warehouses, a natural spring (Ramallo Asensio and Murcia Muñoz 2010), and several paleo-seabed contexts from different

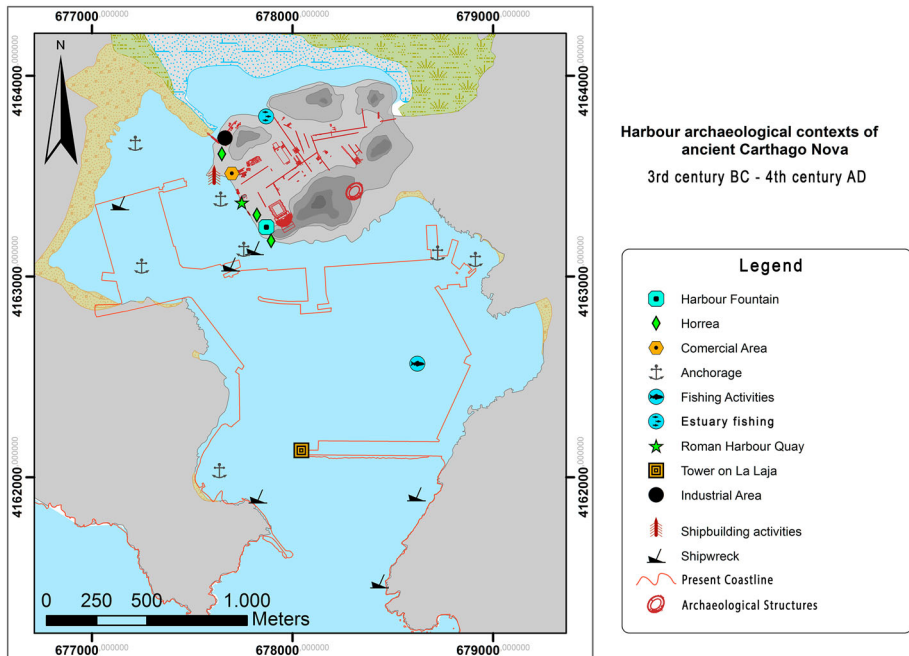


Fig. 2 Archaeological evidence (underwater and terrestrial) of harbour activities in ancient Carthago Nova

historical periods (Cerezo-Andreo 2017). This archaeological evidence reveals a waterfront with intense maritime activity, but without clear protection from south-easterly waves.

However, during the Late Roman period the most frequent anchorage was outside the Mandarache area, in the small cove of the **Espalmador (Fig. 1, #7)**, where underwater archaeological excavations have revealed its importance (Arellano Gañan et al. 1997). It is possible that this displacement was caused by the problem of access to the Mandarache area which had silted up.

One feature that no longer exists but must have had a significant influence on the way the harbour area was used is **La Laja Island (Fig. 1, # 6)**. At the end of the nineteenth century, it was dynamited in order to make access to the harbour easier for steamboats. Currently, one of the Cartagena port lighthouses is located where this small island once stood, and it is now connected to the mainland by a long quay. Due to these changes, many researchers have tended to disregard the role it may have played in the past as an essential feature of the maritime landscape of the harbour.

Several shipwrecks have been identified on the eastern shore of the harbour basin and in the area around **Escombreras Island (Fig. 1, #5)**. Underwater surveys in both areas (Pinedo Reyes 2012) have revealed a great deal of archaeological material embedded within rocky and sandy seabed bottoms, which have been significantly affected by erosion due to the wave energy in that area. However, in the western sector of the harbour the shipwrecks documented were buried in clay and silt sediments, which is typical of areas affected by marine dynamics of lower energy (Mas 2005). These two types of harbour sediments are significant for any understanding of these sites and anchoring activities. The evidence suggests that the shipwrecks found on the rocky seabed, in an area of wind-wave exposure, were the result of misfortunes such as running aground or storms, and not directly related to anchoring

activities, while those found on the silty sediments were the result of events such as collision, fire or simply abandonment.

Climatology, Oceanography, and Paleo-bathymetry

As this study aims to analyse the anchoring activities on ancient Cartago Nova, we have conducted a climatological and oceanographical study after the historical and archaeological research in order to define the data that will be used on the SWAN model.

Cartagena is located in the south-western Mediterranean, at the north-eastern spur of the Alborán Sea where eddies with Atlantic Surface Water enter the Mediterranean (La Violette 1990; Heburn and La Violette 1990; Viúdez et al. 1996a, b). In this section, a description of the current climatology, oceanography, and paleo-bathymetry in the area is provided together with a synoptic description of the model used to hindcast wave propagation in the harbour with different wind scenarios.

Wind

The local high topography provides the harbour of Cartagena with shelter from wind coming from almost any direction except from the south. Figure 3 shows the wind rose obtained from two different meteorological stations: the first, for the boundaries interpolation data, on an oceanographic buoy located 33 nm east of Cartagena (0.33° W, 37.65° N); the second, for the nested model, on Bastarreche dock (0.97° W, 37.57° N) inside Escombreras Cove (Fig. 1, #4) (Puertos del Estado 2017a, b). According to recent historical records by Puertos del Estado (2017a), the Cape of Palos oceanographic buoy that provided data from 2006 to 2014 in the open sea off Cartagena, NE and SW winds from 4 to 6 m/s prevail (50% occurrences), with probabilities not exceeding 6 m/s and 12 m/s of 70% and 97%, respectively, and 16% calm. As you approach the harbour (Escombreras meteorological station), the occurrence of NE winds becomes 24%, while SE becomes 17% and SW 13%. Here, the probability of winds not exceeding 6 m/s is 80%, whereas the probability of those greater than 12 m/s is 99%, with 12% calms (Puertos del Estado 2017a).

These wind patterns are consistent over large timescales—much longer than the 2200 years considered here—as they are forced by the subtropical anticyclone. This anticyclone produces clear skies and high temperatures in summer when it comes from the poleward extension over the oceans; meanwhile in winter, when the anticyclone moves towards the Equator, it is replaced by a travelling frontal (Davis et al. 1997).

Although it is clear that interannual and decadal oscillations in climate exist, they would not substantially affect wind-wave directions and heights in our case. In fact, according to Arnaud (2005), the impact of climate changes on synoptic conditions for our historical period of study in the southeastern Iberian Peninsula is defined by a progressive rise in temperature arriving at the Roman Climatic Optimum (Sánchez-López et al. 2016) between 300 BC and AD 400, and an increase of rain and short dry periods (Calmel-Avila 2014). This can explain periods of high-energy storms, but wind instability seems to be more frequent during the Holocene climate oscillation (Little Ice Age, LIA, fourteenth–nineteenth centuries AD for our region) (McDermott, et al. 2001; Rodrigo 2018; Barr et al. 2019). The general littoral dynamics affected by wind waves: sandbars, coastal sedimentation, coastal progradation, and other geological markers, show general stability in currents and wave direction.

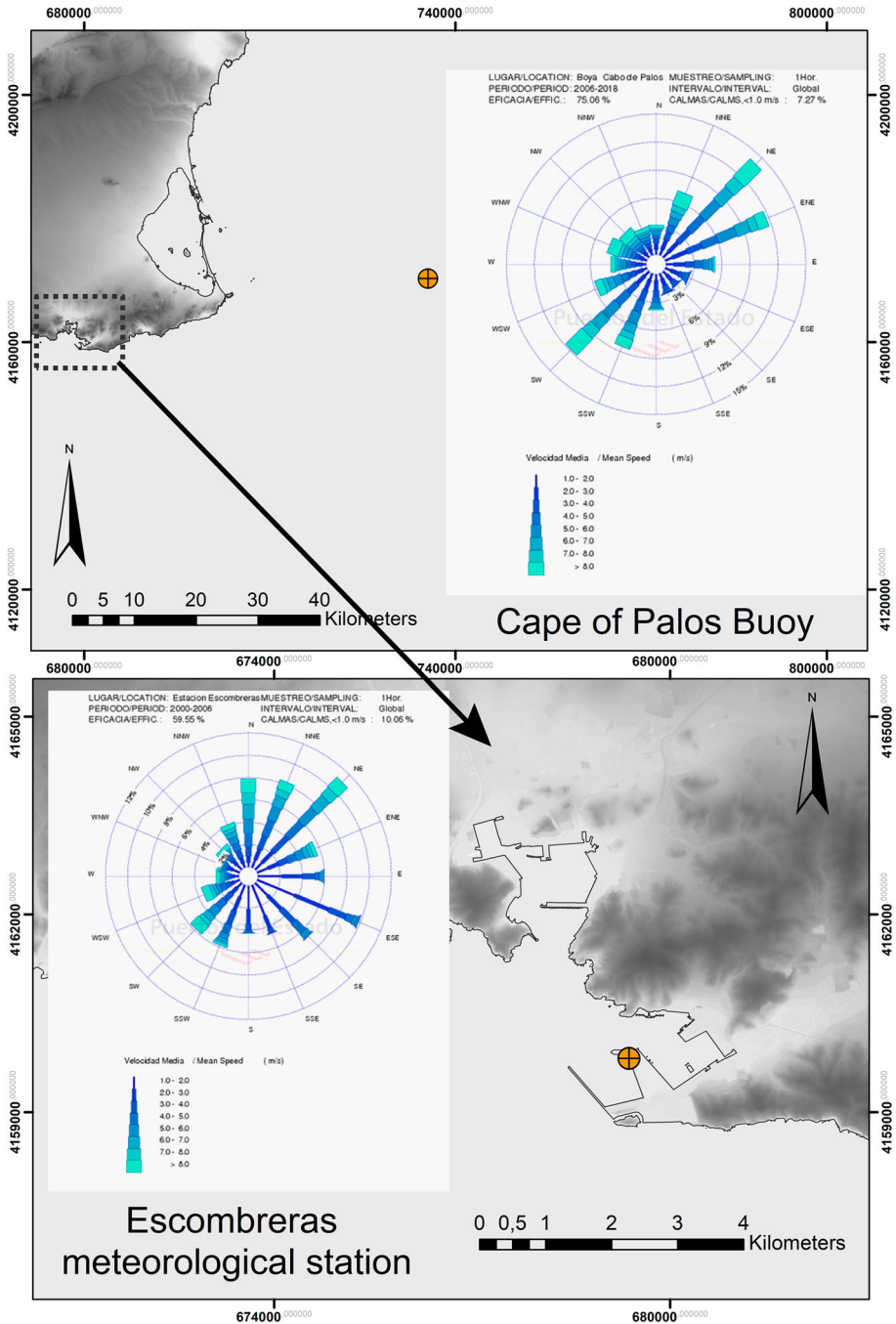


Fig. 3 Location of the meteorological stations recording historical current data with wind roses for the 2006–2017 period. (Source Puertos del Estado 2017a, b, c)

Written sources referring to the arrival at the Roman Climatic Optimum indicate progressive improvement of the weather conditions and stabilising wind dynamics for longer periods (Beresford 2013; Pryor 1995). Hesiod (seventh century BC, Hes. *WD* 619–694) implies that the sailing season in the Mediterranean—later referred to as the *mare apertum*—only lasted for 3 or 4 months in total, a period from the middle of August until the end of September and some time in the spring, although this was more unreliable. Apuleius (second century AD, *Apul. Met.* 11.16) notes a period lasting from March through November for Mediterranean sailing.

The changes in climate during the Holocene affect the length of the optimal period for navigation, but wind-wave direction does not seem to be affected, only the recurrence of storms and wind instability. If these warm and optimal climatic periods are consistent and our analysis of the climatic conditions is coherent, it can be assumed that the data are valid for analysing ancient navigation (Ljungqvist 2010). In this case, the Roman Climatic Optimum period is consistent with this study, from 300 BC to AD 400.

All models in this study take into account the information regarding sea-level change and changes in coastal geomorphology. They have been produced based on the findings of the geoarchaeological study of the harbour (Cerezo-Andreo 2016, 2017; Manteca et al. 2017; Torres et al. 2018). As a result of these studies, data show that sea level has not undergone aggressive changes; rather, during the last 2300 years, it has had a progressive advance from –1.25 m below sea level for the Punic era, up to its current level.

Waves

Ideally wave height, as a measure of its energy, is determined by wind fetch, speed, and duration. However, other parameters can influence wave height such as seabed depth and interaction between obstacles and between waves themselves. Short waves are considered those independent of depth, while long waves are depth dependent. Other parameters such as crosswinds, waves reflection, and refraction due to collision with obstacles also have an influence by transferring energy from one to another, thus producing the real height of waves.

The Atlas of the Mediterranean Wind and Wave Climatology (Stefanakos et al. 2004a, b; WRC 2004; Cavaleri 2005; Cavaleri et al. 1991; Liste et al. 2004; Sánchez-Arcilla et al. 2008) and the Atlas of Wave Climate on the Spanish Coasts (MOPT 1992) are available. According to Cavaleri (2005), there are several sources available which validate these atlases: buoys, satellites, and numerical models. To characterise the wave field, data were used from buoys and models as described below. No satellite observations were used for this study's purpose due to the low spatial resolution available.

Waves recorded at Cape of Palos buoy (Puertos del Estado 2017c) are characterised by an average height of 1 m and peak period of 5 to 6 s and two dominant directions ENE (45%) and SW (20%) (those with more than 50% occurrence). The probability of exceeding an average wave height greater than 3 m is 0.02, with winter months producing a greater probability of exceeding this height. The annual probability of waves exceeding 3 m in extreme episodes is 0.99. The main directions for these extreme waves are NE, E, and SW. The recorded data do not show significant differences between swell and wind waves at this station (MOPT 1992). JONSWAP spectrum theoretical values (Hasselmann et al. 1973; Houmb and Overvik 1976), obtained from the Atlas of Wave Climate on the Spanish Coasts (MOPT 1992), are shown in Table 1.

Although no direct wave measurements have been recorded closer to the harbour of Cartagena, waves in the area are described as the wave operational forecast system for Spanish

Table 1 Theoretical values of JONSWAP wave spectrum off Cartagena

Instrumental data: wave height/period correlation for storms								
$P = H_s/L \bar{p}$	T_P/\bar{T}	Final relationship			Design values			
		H_s (m), T_P (s)			H_s (m)	T_P (s)		
Cape of Palos buoy (Source: Puertos del Estado 2017a, b, c)								
0.035–0.06	≈ 1.20	$T = (3.9 - 5.1)\sqrt{H_S}$			4	7.5–10		
					6	9.5–12.5		
					8	11–14.5		
Instrumental data: basic frequency spectrum for storms ($H_s \geq 1.5$ m)								
H_s (m)—2.5			TP (s)—9.15			γ —3.30		
Theoretical JONSWAP spectrum parameters								
$\bar{\gamma}$	γ_{\max}	γ_{\min}	σ_γ	\bar{f}_p	$f_{p\max}$	$f_{p\min}$	σ_{f_p}	N
3.2	6.3	1.4	1.24	0.13	0.15	0.10	0.014	18

γ is the peak enhancement factor, σ is the standard deviation, f_p is the spectral peak frequency, H_S is the significant height, T is the period, T_P is the peak period and n is the number of storms under consideration.

coasts—managed by Puertos del Estado (2017c; Carretero et al. 2000; Gómez Lahoz and Carretero Albiach 2005)—which provides, along with a network of nodes² (SIMAR network), wave parameters for each node. The operational system is based on a WAN version developed for deep waters (WAMDI Group 1988; Komen et al. 1994) and a nested Simulating Waves Nearshore—SWAN model (Booij et al. 1999; Holthuijsen et al. 2004)—for shallow waters (Wolf et al. 2000). This system is validated by the network of buoys measuring waves near real time (Guillaume et al. 1992; Gómez Lahoz and Carretero Albiach 2005), as part of the European Centre for Medium-Range Weather Forecasts (ECMWF 2017).

In this study, SIMAR node 2071090 (1.08° W, 37.50° N) 6.6 nm off Cartagena harbour (Fig. 4) is used to characterise waves near the harbour entrance. According to these data, the average (80% of occurrence) wave height is less than 1 m and peak period between 5 and 6 s, with predominant directions of origin being E (40%) and SSW (30%). The probability of a wave height greater than 3 m occurring is around 1% per year, with greater probability in winter. The percentage of calms is 10.20%.

Comparing the wave directions of the Cape of Palos buoy and near the harbour entrance (SIMAR node 2071090), it is possible to observe how the protective effect of the coast almost makes the waves coming from the NE disappear altogether, thus suggesting that NE winds are responsible for wind waves only, while those of the other directions would be a combination of swell and local wind effects.

Paleo-bathymetry

The paleo-topographical reconstruction of the harbour has been carried out based on the selection of 21 geophysical cores at key points in the current topography of the city. ¹⁴C dating was carried out on the organic material within these cores and validated through the appli-

² See data online on <http://www.puertos.es/es-es/oceanografia/Paginas/portus.aspx>, last accessed in December 2019.

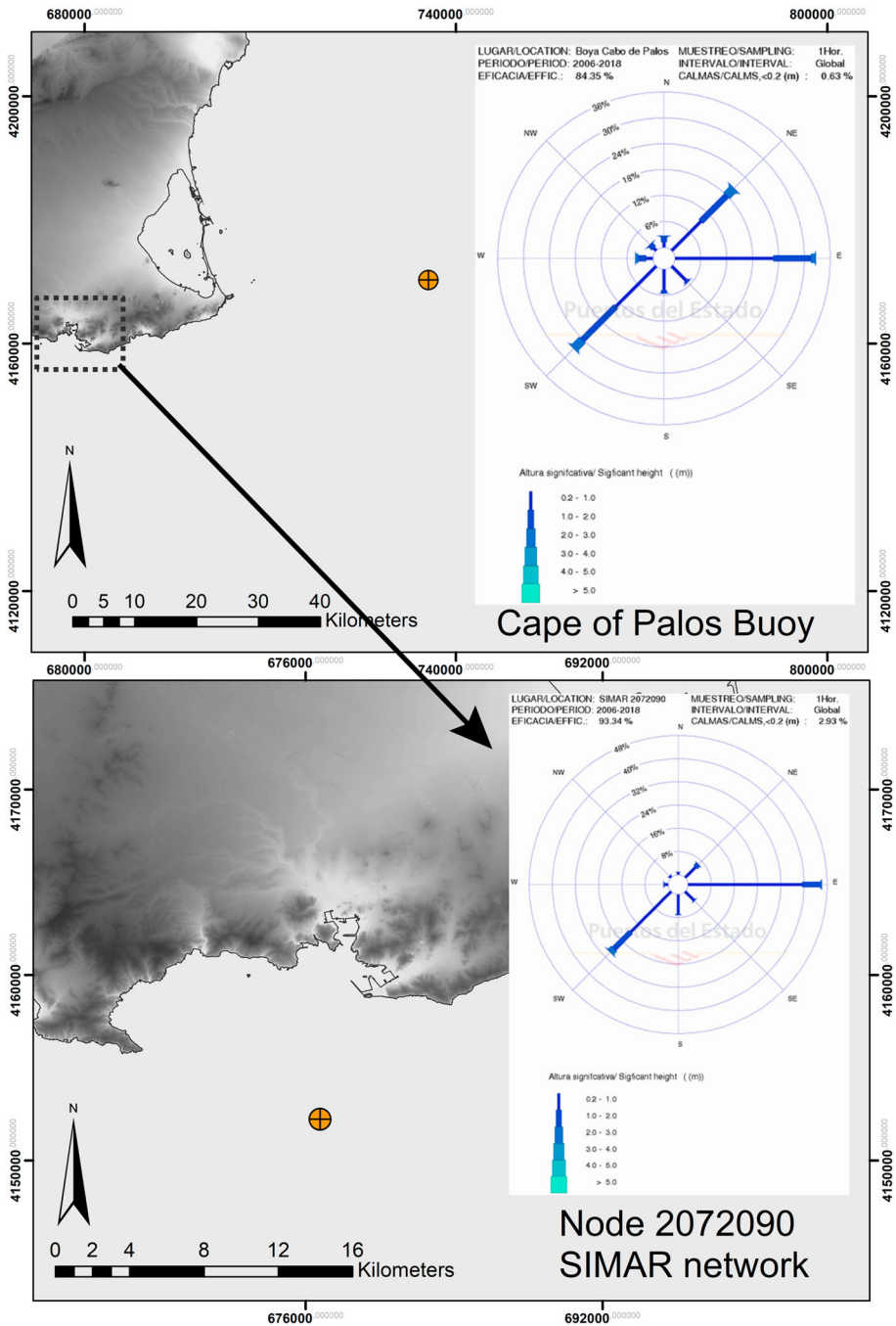


Fig. 4 Location of the meteorological stations recording historical current data with wave roses for the 2006–2017 period (Puertos del Estado 2017c)

cation of amino acid racemization techniques (Ortiz et al. 2015). Several biomarker studies (Torres et al. 2018), as well as other archaeometric and geomorphological studies, permitted the proposal of diachronic reconstruction of the paleo-topography of the environment for a period of over 12,000 years (Manteca et al. 2017).

Concerning the coastline, it is very irregular with a constant succession of rocky cliffs and small sandy or gravel coves. The Harbour of Cartagena (Fig. 1, #5) is practically surrounded by a rocky and vertical coastline with small beaches like Espalmador (Fig. 1, #7), Santa Lucia (Fig. 1, #6) or San Julián (Fig. 1, #14). Only on the northern and western shore of the Mandarache (Fig. 1, #3), more extensive sand beaches can be found. All this landscape is now destroyed by the contemporary harbour, and shores have been restored using historical cartography (Cerezo-Andreo 2016; 178–200) and information derived from cores (Torres, et al. 2018). The evolution of these beaches can be traced in Fig. 6.

The importance of seabed roughness for wave development in shallow water is well documented (Barua 2017; Moghimi et al. 2005). For this purpose, the previous data mentioned were used, as well as the joint use of spatial analysis with GIS for the interpolation of paleo-bathymetric isobath. The findings from geoarchaeological and underwater archaeological studies (Miñano Domínguez and Castillo Belinchón 2014) have been used to identify apparent sedimentation rates in the different harbour sectors (Salomon et al. 2016). The estuarine sector of the Mandarache (Fig. 1, #3) is affected by a higher rate of sedimentation than the eastern sector of the harbour area and the south-western area of Espalmador (Fig. 1, #7). ^{14}C dating of the cores, archaeological information, and historical cartography were used to reliably interpolate the paleo-bathymetry. Age models were calculated from these data (Blaauw 2010), which when compared with the chronostratigraphic information of the cores, allowed for the establishment of variable sedimentation rates for the different periods to be modelled (Fig. 5) (Giaime et al. 2017).

Once the sedimentation ratios had been established, a network of historical cartographic bathymetric data was used to perform several interpolation tests with GIS. By comparing data from 120 historical maps, it has been possible to establish common bathymetric points on 25 of them, most of which date from the eighteenth and early nineteenth centuries. This allowed for the establishment of a network of more than 370 common bathymetric points, with a spatial resolution of one point every 10, 20, or 30 m depending on the scale (Cerezo-Andreo 2016: 367–419). These data provide the means to identify patterns of sedimentation; for example for the period 1721 to 1746, a natural sedimentation process of 15.2 mm/y in the Mandarache area and one of 1.6 mm/yr in the outer harbour area were verified.

Taking into account this duality in patterns of sedimentation over time, the results of the age models and the harbour contexts strata of the cores along with the findings from underwater archaeological investigations have been used to obtain sedimentation ratios for our three periods of this study: (A) the Punic period (third century BC), (B) Late Roman Republican period (first century BC), and (C) Late Roman period (fourth century AD). This methodology was used for the other two control models: (D) the middle of the eighteenth century and (E) the present day, in order to ascertain whether the evolution of the process of sedimentation was coherent and consistent. These paleo-bathymetric models were used to perform the wave hindcasts (A–D shown in Fig. 6).

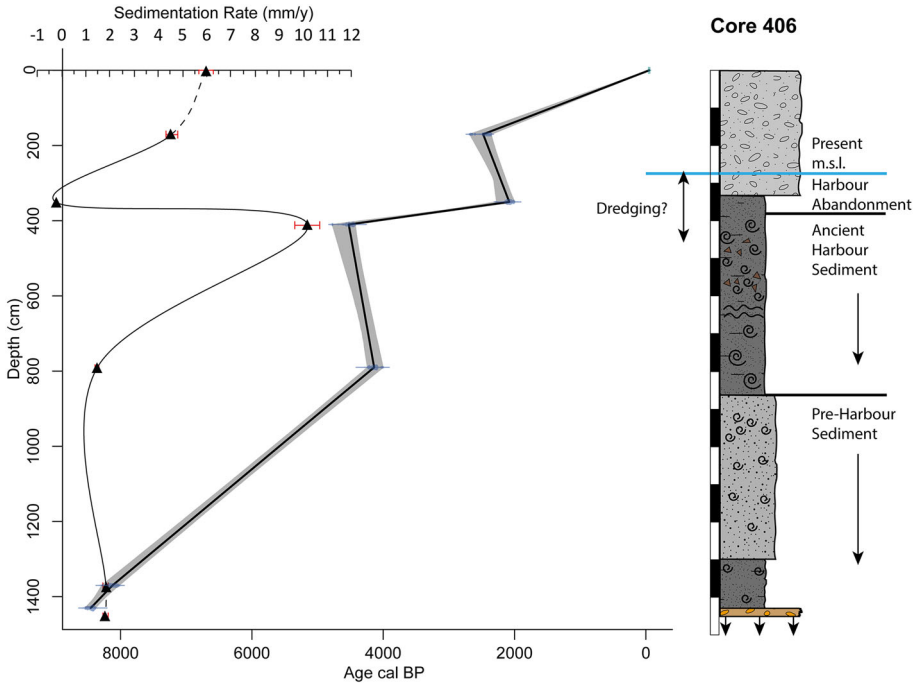


Fig. 5 Example of the process for reconstructing the paleo-bathymetry through age-depth model, sedimentation rates, and archaeological data. Core 406 location is equal to Fig. 1, #9. Data Source ARQUEOTOPOS Project: Torres et al. 2018, Manteca et al. 2017, and Cerezo 2016

Wave Modelling

Sea-level variations due to waves are the sum of different processes such as generation (wave growth caused by wind), propagation (shoaling, refraction, reflections, and diffraction), transformation (nonlinear wave–wave interactions), and dissipation (wave breaking, whitecapping, and bottom friction). Wave models calculate the wave energy spectrum (E) as a function of space (x,y), time (t), frequency (f), and direction (θ) as:

$$\frac{dE(x,y,t,f,\theta)}{dt} = S_{in} + S_{nl4} + S_{wcap} + S_{nl3} + S_{br} + S_{bot}$$

}
 Deep water terms

}
 Shallow water terms

where S_{in} is the wind effect, S_{nl4} and S_{nl3} the nonlinear wave-wave interactions, S_{wcap} the whitecapping, S_{br} the depth-induced breaking, and S_{bot} the bottom friction.

According to the way the wave models solve the nonlinear processes, they can be classified as *first-generation models* (those that do not have an explicit nonlinear term), *second-generation models* (those handling the S_{nl} term by parametric methods, for example by applying a reference spectrum to reorganise the energy over the frequencies), and *third-generation models* (those calculating the nonlinear energy transfers explicitly). This study uses the third-generation model Simulating WAVes Nearshore—SWAN—(SWAN Cycle III version 41.01AB) developed by Delft University of Technology and widely used worldwide.

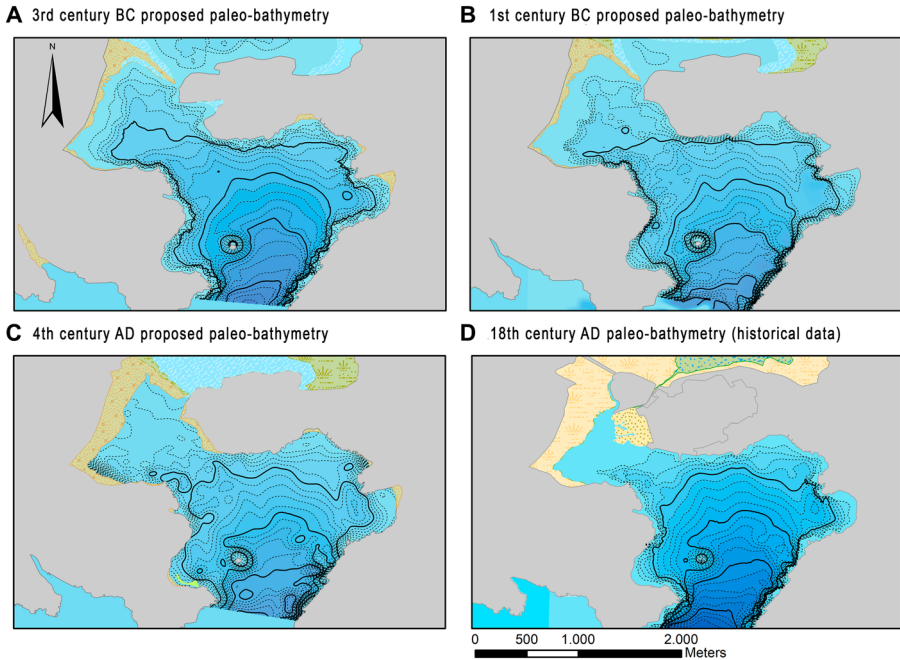


Fig. 6 Proposed paleo-bathymetry for the three modelled time periods A-C. Model D: historical bathymetry from cartographic data. Model E, present-day model, not shown. 1 m contours

SWAN Model

SWAN is a derivation of the previous WAM model (WAMDI Group 1988; Komen et al. 1994). WAN is based on the spectral description of the sea surface, i.e. at all points of the grid covering the area of interest the wave conditions are represented as the superposition of a finite but large number of sinusoidal components, each characterised by frequency f (Hz), direction Θ_m (flow, degrees), and height h (m); hence energy F proportional to h^2 . The evolution in time and space of the whole field is governed by the so-called energy balance equation:

$$\frac{\partial F}{\partial t} + Cg \nabla F = Sin + Snl + Sdis$$

where the terms on the left represent the time derivative and the kinematics of the field and those on the right the physical processes at work for its evolution. More specifically, $\partial/\partial t$ is the derivative with respect to time; Cg is the wave group speed; and ∇F represents the spatial gradient in the field. The energy input by the wind, Sin term, is provided by the driving wind fields. The fourth-order nonlinear transfer due to resonant wave-wave interactions, Snl , represents the conservative exchange of energy between the different wave components that take place continuously. The dissipation term, $Sdis$, summarises the energy loss by the various dissipation processes at work: whitecapping and turbulence (WAMDI Group 1988).

The SWAN model includes shallow water source terms such as depth-induced breaking and triad wave-wave interactions, also taking into consideration the wave energy dissipation by turbulent interaction (Booij et al. 1999; Holthuijsen et al. 2004). It is a numerical wave model for wave simulation in coastal areas from given winds and depths and geomorphologi-

Table 2 Wind scenarios modelled for each time period

Scenario	Wind direction	Degrees	Velocity m/s
A	SSW	212°	13.4
B	SSW	202.5°	4
C	SE	135°	7
D	NNE	22.5°	5
E	S	180°	4

cal conditions. The model is based on the wave action balance equation (or energy balance in the absence of currents) representing the following wave propagation processes: (1) propagation through geographic space; (2) refraction due to spatial variations in bottom and current; (3) shoaling due to spatial variations in bottom and current; (4) blocking and reflections by opposing currents; and (5) transmission through, blockage by or reflection against sub-grid obstacles.

The following wave generation and dissipation processes are also represented in SWAN: (1) generation by wind; (2) dissipation by whitecapping; and (3) dissipation by depth-induced wave breaking.

SWAN was executed with the following options: “gen3” (to run it in third-generation mode for wind input, quadruplet interactions, and whitecapping); “breaking” (to influence depth-induced wave breaking in shallow water); and “diffract” (to include diffraction in the wave computation).

Wind Forcing

Five scenarios based on different winds were simulated for each bathymetry (bathymetry and coastlines of Fig. 6) according to the following criteria: (1) winds of higher than 48% of frequency (SSW—212° and 202.5° and NNE—22.5°) (scenarios B and D); (2) the wind shelter role of both Escombreras Island and La Laja Island with S (180°) and SE (135°) winds (scenarios C and E), which have a direction towards the harbour entrance although with a lower annual occurrence (3% and 5%, respectively); and (3) an extreme wind case (scenario A) producing the highest wave discovered during the time period analysed (2012–2016) at the SIMAR node 2071090, with 4.40 m wave height (predicted for January 2013 with SSW (212°) direction and 13.4 m/s wind speed). Table 2 shows the simulated scenarios with direction and wind velocity.

Besides the effect of local winds, swell must be taken into account to simulate the wave-field. To do this, the boundary conditions included wave height, direction, and period from the Puertos del Estado operational model, which includes also the swell in the area of study. The selected SIMAR network node for taking the boundary conditions was number 2072090 (1° W, 37.50° N). Additionally, a comparison between two other SIMAR nodes—located to the west (node 2071090, 1.08° W, 37.50° N) and east (node 2073090, 0.92° W, 37.50° N) of the domain area for our model—showed a very slight variation of the waves, thus confirming a homogeneous swell along the boundary contour of the model.

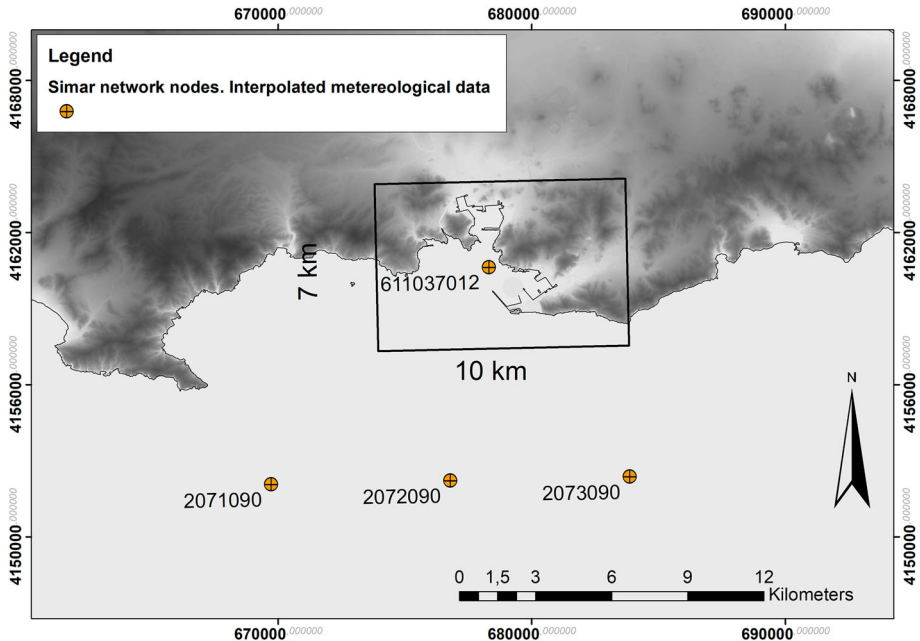


Fig. 7 Location of the domain for numerical simulations and SIMAR network nodes for boundary data

Horizontal Discretization

Figure 7 shows the SWAN model domain traced to make sure the model reflected the morphological variability of the coast over the period of time analysed as well as the bathymetry. The spatial resolution was set at 13×16 m to ensure it captured the effects of Escombreras Island and La Laja Island and adjusted optimal time-step. Bathymetry was interpolated to this spatial resolution with a 1 m contour.

Model Confidence

The simulation was conducted with the current morphology and bathymetry of the harbour of Cartagena to evaluate the validity of the simulations. Results were compared with those from the SIMAR node 611037012 (0.98° W, 37.58° N), located inside the simulated area (Fig. 7), using the same winds. The coefficient of determination (r^2) between them was 0.99 for wave height and 0.96 for both direction and period.

Wave height and period are the main parameters determining anchorage places, particularly the highest with shorter periods. Generally, data derived from the archaeological research on shipwrecks from the period in question indicate that ships had a low relation between draught and deadrise, generally no higher than 60 or 90 cm (Boetto 2010:118; Poveda 2015; Salomon et al. 2016: Fig. 5). A vessel of these characteristics anchored and subjected to a constant dynamic of waves greater than 0.6 m would have problems in maintaining its stability, or remaining safe if we take into account the tension and constant distension of an anchor rope made of vegetable fibre.

ASI—Anchorage Safety Index

In order to determine the safest places to anchor in the reconstructed harbour, an analysis was made using map algebra in ESRI Arc Map software. A classification of paleo-bathymetry raster data was performed in three categories according to anchorage limits proposed for ancient ships: a) 0 to -1.25 m below sea level, depth not suitable for anchorage; b) -1.25 to -10 m below sea level, maximum depth of anchorage; and c) below -10 m below sea level.³ After this classification, the categories a) and c) have been removed, assigning to class b) the numeric value 1. Thus, value (class b) is used to identify the areas with an optimal depth according to draught and accessibility for anchorage. This is the Raster Anchorage Limit (RAL). With the Raster Calculator Tool, the medium wave height provided by the predominant annual wave scenarios was calculated. The result of medium wave regime (MWR) is classified by three categories of wave height: >60 cm, very bad or risky anchoring; from 30 to 60 cm regular or intermediate anchoring; <30 cm secure anchoring. The raster data resulting (MWR) were multiplied by the RAL, resulting in a new raster that shows potentially optimum zones for anchoring according to two key conditions: wave and draught. This resulting raster is defined as the Anchorage Safety Index. Thus, it is possible to evaluate aspects of security and accessibility and contrast them with findings from archaeological anchorage data.

Results

Wave Model Hindcast for the Punic Period—Third Century BC

Figure 8 shows the numerical wave simulations with prevailing winds in the area (Table 2) around 250 BC. Here, scenario E (with SE winds— 180° , 4 m/s) is not shown since it did not return relevant results due to its low occurrence (below 5%) and speed.

Scenario A (Fig. 8A) simulated with SSW (212°) winds—regionally known as *Leveche*—of 13.5 m/s (Table 2) is one of the most frequent storms—over 12%—in the area. It is noteworthy that waves between 2 and 3.5 m in height and 5–6 s period entered the harbour reaching the waterfront of the southern part of the peninsula, but not the *Mandarache* and the *Espalmador* areas. Only 17% of the space inside the harbour had waves of less than 0.5 m in height, and, importantly, the *Mandarache* and the *Espalmador* areas and the cove of the waterfront of the ancient city and the beach of San Julián were the only spaces with calm waters when these weather conditions prevailed.

Waves outside the harbour could reach heights of over 4.5 m, meaning that winds and waves could push boats towards *Escombreras* Island. In these conditions, it would not be so easy to reach the interior of the harbour through the mouth. Most probably vessels would be able to reach *Escombreras* Cove, with its steep cliffs that are a risk for approaching and anchoring.

³ For more information about ancient ship draught, see Poveda 2015, Pomey and Tchernia 1978, de Juan 2013 and Boetto 2010. According to these authors, wave heights of 50 or 60 cm and depths shallower than -1.25 m are considered too risky for anchorage. Common nautical knowledge on sailing (see also Morton 1998; Beresford 2013: 229) does not recommend anchoring at depths greater than -10 m, as there is too much anchor line to pull up in a short time in case emergency. Another important factor for anchoring is related to the seabed type; sand or silt sediment is preferred over a rocky one for anchoring. In a rocky area, the anchor could get stuck.

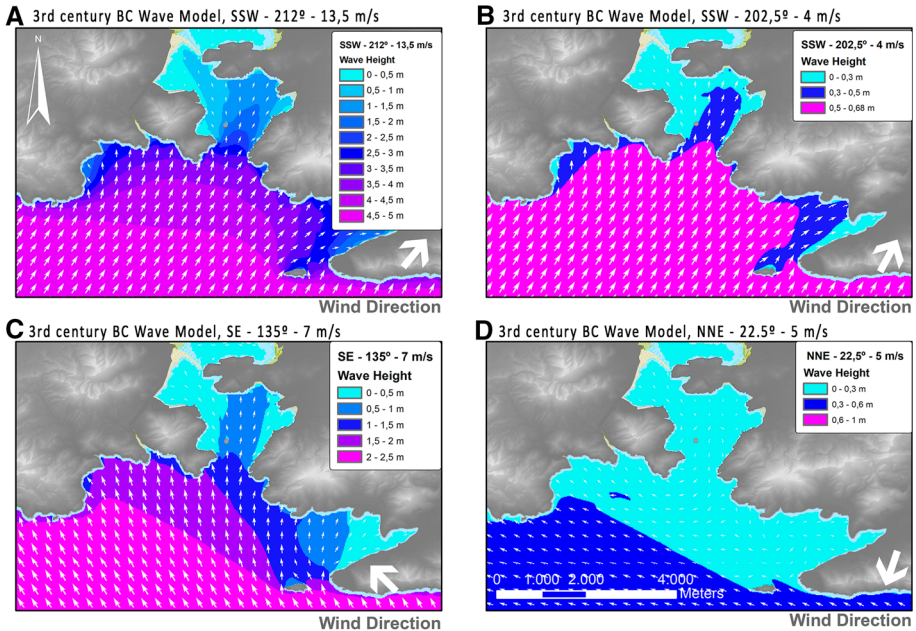


Fig. 8 Wave modelling of the bay and harbour of Carthago Nova. Reconstructed paleo-topography by ARQUEOTOPOS Project. Wave height classification each 0.5 m on output model scenarios A and C, each 0.3 m on output model scenarios B and D. Small white arrows represent wave direction. White bold arrows highlight general wind direction

Scenario B (Fig. 8B), with SSW winds at 4 m/s, is by far the most common scenario (36% occurrence throughout the year). Here, wind waves are much smaller, up to 0.65 m at the mouth, with waves from 0.3 to 0.5 m entering through the mouth but not arriving at the coast, thus leaving an area in front and at both sides of the city's waterfront with lower waves (up to 0.03 m height).

The SE winds (135°) of 7 m/s used to simulate scenario C (Fig. 8C) are less frequent (16% occurrence) than those for scenario B (Table II), although they are the most common component of the coastal breeze system at sunset. Waves reach more than 1.5 m height at the mouth of the harbour and reach 0.5–1 m at the city's ancient waterfront. Here, the wavefield entering the harbour separates into two areas of lower waves at both sides east and west. The wave map also shows clearly the sheltering effect of Escombreras Island in these conditions. The role of La Laja Island is only significant for the western part of the harbour space.

The last scenario, D (Fig. 8D), with NNE wind of 5 m/s and 37% occurrence in spring and summer, confirms that this weather does not affect the nautical synoptic conditions of the bay, making it easier for the vessels to leave.

Wave Model Hindcast for the Late Roman Republican Period—First Century BC

Figure 9 shows the wave simulations with the prevailing winds (Table 2) in Carthago Nova harbour in the first century BC (around 70 BC) with a different coastal topography after years of coastal progradation and sedimentation. The Mandarache is shallower than in the third

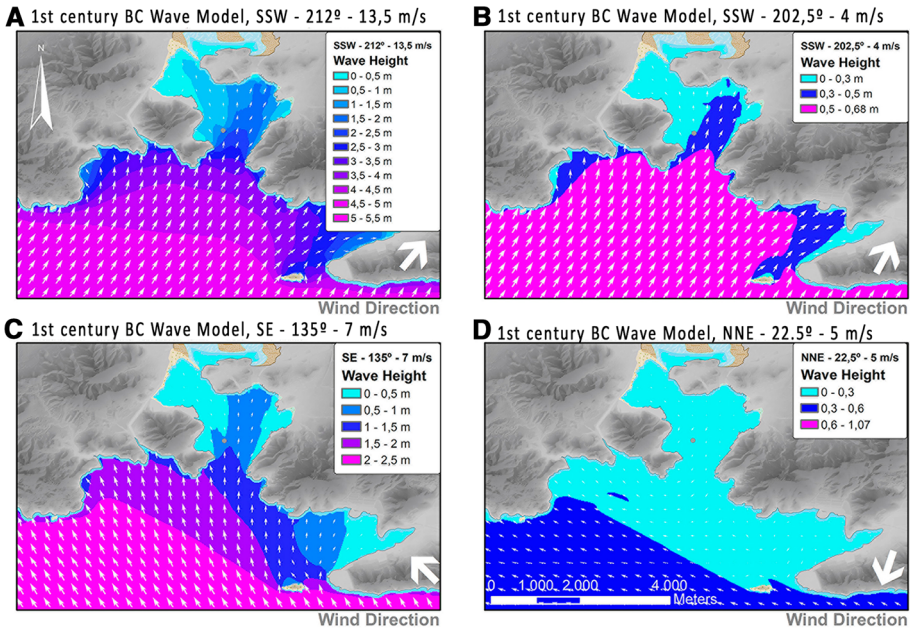


Fig. 9 Wave modelling of the bay and harbour of Carthago Nova. Reconstructed paleo-topography by ARQUEOTOPOS Project. Wave height classification each 0.5 m on output model scenarios **A** and **C**, each 0.3 m on output model scenarios **B** and **D**. Small white arrows represent wave direction. White bold arrows highlight general wind direction

century BC, the cove at the waterfront of the ancient city is almost silted in, and beaches in the eastern sector of the bay are affected by wave propagation.

Scenario E (with SE winds— 180° , 4 m/s) is not shown since it did not return relevant results due to its low occurrence (below 5%) and speed.

Results for scenario A (Fig. 9A) (SSW 212° —13.5 m/s wind speed) show that during storms, the period between waves decreases and their height increases, producing waves between 1.5 and 2 m high in the eastern sector and waves between 0.5 and 1.5 m high on the waterfront of the ancient city, without any shelter for boats anchored there. The only spaces with calm waters in these weather conditions were Espalmador and the western sector of the Mandarache providing 20 ha of safe anchorage. Scenario B (Fig. 9B) shows smaller wind waves, maximum of 0.68 m high also at the entrance of the harbour, and generally with minimal effect on anchorage areas and the waterfront. Nevertheless, in some areas, a low wave height increase can be detected. Scenario C (Fig. 9C), with stronger winds (SE 135° —7 m/s), shows that during this period, Escombreras and La Laja Islands played a significant role decreasing wind waves entering the western area and the Mandarache anchorage area. Waves reach a height of 1.5 m at the mouth of the harbour and reach 0.5–1 m in the eastern sector of the bay.

The high incidence of scenarios B and C, 52% jointly throughout the year, makes it possible to assess the safety of the anchorages from the perspective of long term trends. In this sense, according to the simulated data the safest anchorages for this period were the Mandarache and Espalmador, in the western sector of the bay.

As for the previous chronological phase, scenario D (Fig. 9D), with 37% occurrence in spring and summer, confirms the general safety of the area during the *mare apertum* season.

Wave Model Results for the Late Roman Period—Fourth Century AD

Figure 10 shows the wave simulations with the prevailing winds for the Late Roman period (fourth century AD), where the analysis is adjusted to the evolved paleo-topography and to the considerable sedimentation of certain zones of the harbour area. In this sense, it is noteworthy that the Mandarache was shallower than in the previous time periods, with water depths around an average of -1.56 m below sea level although some deeper areas remain. Scenario E (with SE winds— 180° , 4 m/s) is not shown since it did not return relevant results due to its low occurrence (below 5%) and speed.

This alteration of the bathymetry considerably affects the dynamics of waves by increasing the wave height inside the bay and generating greater instability in all areas. As can be seen in scenario A (Fig. 10A), in the eastern part of the Mandarache the waves reach heights of up to 1 m. This is the Late Roman waterfront of the city where *horrea* have been identified (Cerezo-Andreo 2017). The eastern part of the bay presents waves high between 1.5 and 2.5 m near the beaches. As the waves move towards the anchorage zones, they become more frequent, with periods of 1.2 and 0.74 s between waves. Undoubtedly, this must have affected the management of harbour activity and, consequently, other anchorage areas were sought as seems to be the case of the Espalmador (Fig. 1, #7). Although with weak SE winds (Fig. 10C), the Espalmador area remains problematic.

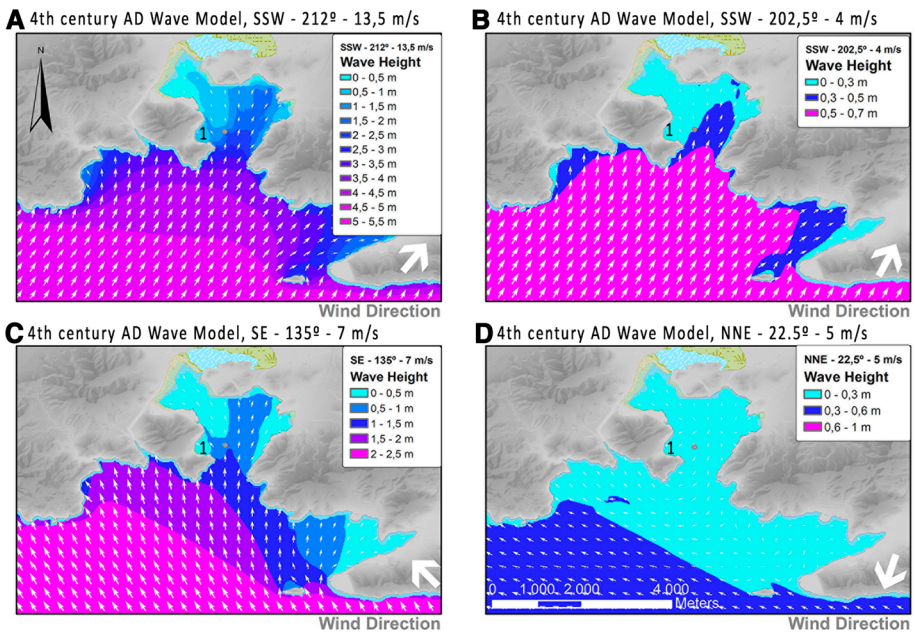


Fig. 10 Wave modelling of the bay and harbour of Carthago Nova. Reconstructed paleo-topography by ARQUEOTOPOS Project. Wave height classification each 0.5 m on output model scenarios A and C, each 0.3 m on output model scenarios B and D. Small white arrows represent wave direction. White bold arrows highlight general wind direction

Discussion

The application of a multidisciplinary methodological approach, taking into account historical, archaeological, and oceanographical data, has provided new insights into a better understanding of the role of the harbour of Carthago Nova in ancient times. Whereas in the previous section waves were hindcasted for three different periods between the Punic and Roman periods (third century BC, first century BC, and fourth century AD), two more recent simulations were performed (eighteenth century AD and present day), both with their respective cartography and topography and the same wind-wave scenarios as above (data not shown). Although these simulations are beyond the scope of this paper, they fitted the descriptions of the synoptic conditions of the time. As mentioned in the section on model confidence, the reliability of the data makes it possible to address several historiographical and archaeological questions in order to understand the role of the harbour in ancient times, as well as analysing how the harbour could be managed.

The Role of Coastal Accidents, La Laja and Escombreras Islands, and Protecting the Harbour

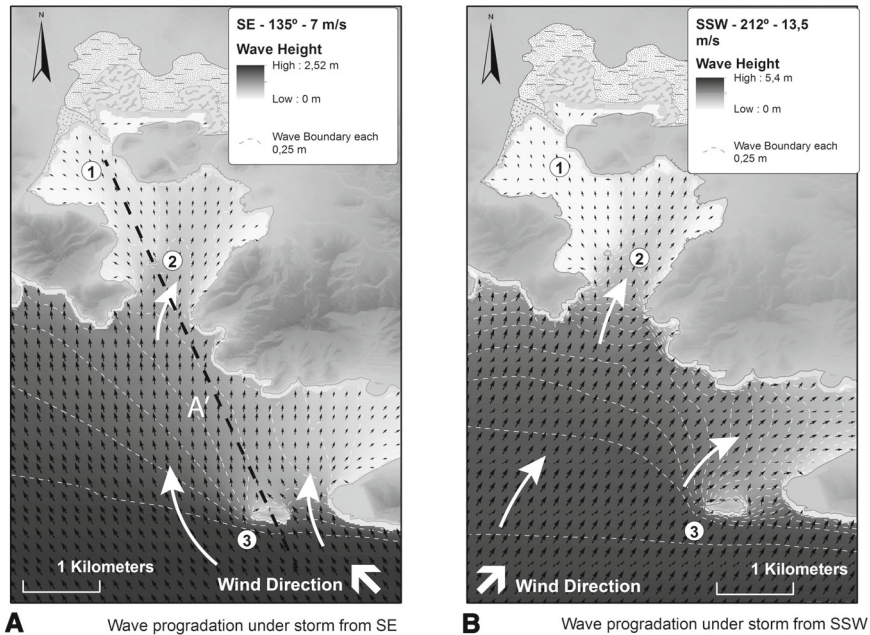
An island is highlighted by several classical authors as the main feature protecting the harbour mouth of ancient Carthago Nova, amongst others Polybius (second century BC; Plb. 10.10), Strabo (first century AD; Strab. 3.4.6), Titus Livius (first century AD; 26.42.8), Appian (second century AD; *Ib.* 20), and Virgil (first century BC, *Aen.*, 1.569-69).

This has remained in historiography as an unquestionable fact, which has only now been analysed (Fig. 11). Traditionally, the island has been identified as Escombreras Island (Fig. 11, #3) following Strachan-Davidson (1888), where the idea of the island as a natural breakwater that would guarantee the safety of boats anchored in the harbour is first proposed and defended (Fig. 11, #1). However, the name of the island is never mentioned in the original ancient texts. The most detailed description is given by Polybius (Plb. 10.10) who notes that there was an island at the entrance of the harbour that generated two access channels. The island broke the force of the waves protecting the rest of the inner harbour.

As the wave map shows (Fig. 11), following the reconstructed coastal topography and bathymetry, Escombreras Island does not have two narrow channels around it, nor does it block the harbour. It is possible that Polybius is referring to another island—La Laja Island (Fig. 11, #2; Fig. 1, #6) that no longer exists, since a breakwater connecting the former island with the eastern coastline was built at the end of nineteenth century.

The wave hindcasting results show that Escombreras Island certainly plays an important role in protecting the bay from waves. With SE winds (135°), at a speed of 7 m/s, this analysis shows the importance of the island (Fig. 11A), as waves of 2.5 m high are reduced to 1.5 m behind the island. Nevertheless, it can be observed that the landscape feature which is important for the security of the harbour space is La Laja Island (Fig. 11, #2). It is from this point when the height of the waves falls drastically and ceases to be a problem for activities in the harbour area. Despite Escombreras Island and the narrow port mouth, it is at La Laja Island where the waves lose height from 2 m to 0.8 m. It is at this point where two narrow entry channels are formed. It is this feature that guarantees the safety of the interior waters of the harbour.

The analysis has permitted the reinterpretation of the information from Polybius and allowed us to understand how, in the harbour management of the ancient Carthago Nova, La Laja Island located right at the harbour mouth was the main natural element safeguarding



A' Profile Graph Wave Height, Scenario A

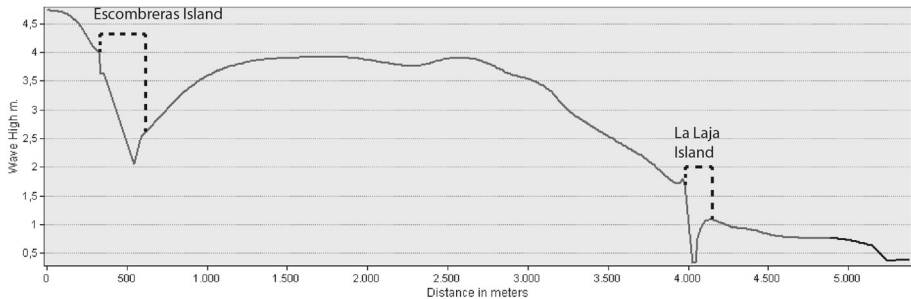


Fig. 11 Wave modelling results for the evaluation of La Laja and Escombreras Islands' role in protecting the harbour at the first century BC. **a** Progression of wave height with SE winds. **b** Progression of wave height with SSW winds. Profile A' wave height profile

the vessels anchored in the harbour. It generated two distinct regimes in the harbour bay: a protected space to the west and an unprotected space to the east. This explains the choice of the Mandarache as the main anchoring zone.

Anchorage and Their Historical Evolution

According to Arnaud (2005) and Medas (2004), waves were one of the most important factors when considering where to anchor an ancient vessel. However, up to the present there have been very few studies carried out that have tried to explore, through mathematical modelling, how waves moved within a harbour area, how this was managed by adding infrastructure, and how it affected vessels (Cibecchini 2008: 484; Millet et al. 2014:201; Safadi 2016: 349).

According to the findings from archaeological research, the maximum wave height that an anchored boat can withstand is 0.60 m (Boetto 2010; Pomey and Tchernia 1978). The freeboard of these vessels with respect to the sea was generally low, and on the other hand, the constant pitch would subject anchor ropes to intense tension which could cause them to break. Three categories have been established to classify the anchoring areas of a harbour based on wave height: > 60 cm, very bad or impossible anchoring; from 30 to 60 cm, regular or average anchoring; < 30 cm, secure anchoring.

Thanks to the data obtained, it is now possible to analyse the evolution of anchoring activities based on ancient topography and wave height: the ASI analysis. In order to do this, the problematic scenario of Leveche storms (SSW—212°—15.3 m/s) has been selected. The aim is to compare simulated results with the data about anchoring activities obtained from findings from terrestrial and underwater archaeological surveys and excavations (Fernández Matallana 2008; Miñano Domínguez 2012; Ramallo Asensio and Martínez Andreu 2010). The ASI analysis makes it possible to increase insight into a very specific area within the wide range of elements that form part of the “maritime cultural landscape” (Westerdhal 2011). Within this landscape of Carthago Nova, these anchorages belong to an area that is influenced by natural elements, that is the effect of wind and wave activity, the physical locations where the ships anchored, and the anchorage archaeological contexts, where concrete material evidence of anchoring activity has been discovered. This is of enormous interest and benefit for furthering our understanding of the relationship between maritime cultures and the sea, and the impact of human activity on the maritime landscape (Ford 2011).

Figure 12A shows the ASI for the Punic period (third century BC), mainly in the space of the Mandarache and in the small cove between the two main hills of the city. This area corresponds with archaeological findings since more than 65% of the Punic anchoring finds (anchors, amphorae, and pottery) derive from this space. However, data from the Santa Lucia area ($\pm 15\%$ of Punic contexts) do not seem to indicate an area where anchoring could be habitually safe.

The results of the analysis (Fig. 12B) for the Late Roman Republican period (first century BC) are even more surprising. Apparently, the Mandarache remains the safest anchoring area, but only 25% of the archaeological finds from this period are situated here. The area of concentration of the Late Republican anchorage evidence is at the ancient waterfront of the city (40–60%), which, on the contrary, does not offer guaranteed anchorage, because at this point the waves arrive at a height of 0.8 m with S–SW winds (13.5 m/s) and 0.7 m with S–SE winds (7 m/s).

This suggests that somehow, during the Late Republican period (first century BC), some kind of artificial structure had to be built out into the water to guarantee anchoring and docking of the boats there. This could be related to a recently discovered Neronian quay with older foundations (Fig. 2, #Roman Harbour Quay) (Torres et al. 2018) and the inscription of a probable breakwater in *opus pilarum* (CIL II 3434).

A structure of this type could explain the aggressive rate of siltation of the waterfront area in the Late Roman period (fourth century AD). As can be seen in Fig. 12C, this silting, causing shallow waters, led to a progressive abandonment of the Mandarache as an area for anchorage. Only 37% of archaeological finds from this period are concentrated in this area. There is a great change in the bathymetry and hydrodynamics of this area, causing the space of the Espalador to become from this moment until the middle of the seventeenth century the main anchorage area of the city.

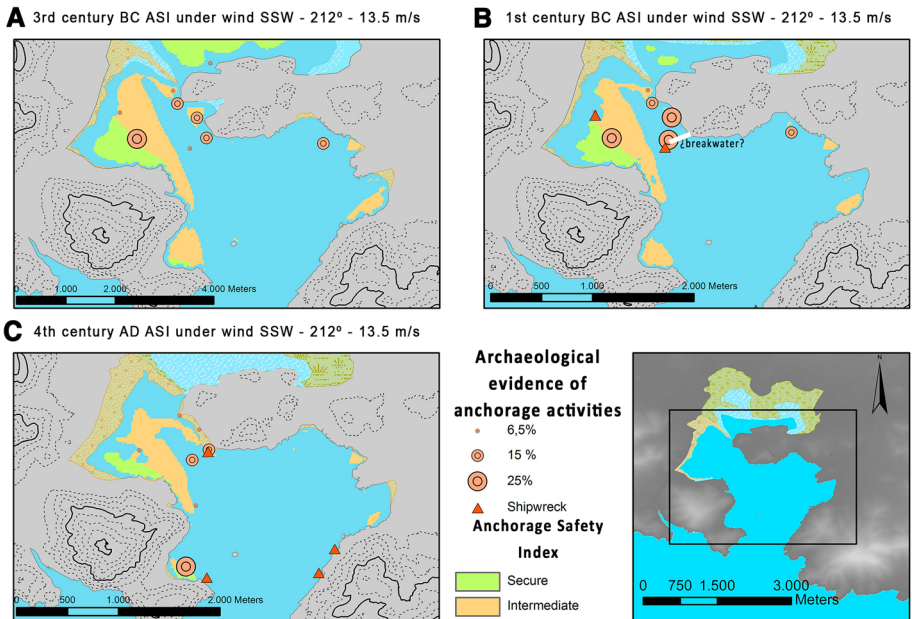


Fig. 12 Spatial analysis of Anchorage Safety Index

Was There a Need for a Breakwater in *Opus Pilarum*?

There remains the question of the existence of an artificial breakwater in Carthago Nova built in *opus pilarum*, around the first century BC, of which we only have probable epigraphic evidence (CIL II 3434). This inscription alludes to a collegium of *liberti* and *servi* who oversaw the construction of a *ex caemento* consisting of *pilas III et fundamenta*. The identification of *pilae III* as part of a port structure, a breakwater or quay, is made by Abascal Palazón and Ramallo Asensio (1997: 71–77), who mostly base their hypothesis on the inscription of Antoninus Pius on this type of construction at Puteoli (CIL X 1641) and on the several of well-known glass flasks of Pozzuoli depicting breakwaters (Ostrow 1979).

The waterfront of the ancient city was affected by wave height during heavy winds from both SSW and SSE, which occurs 18% of the year. The time period between waves in this situation is less than one second, explaining why the constant movement and height of the waves would create a high risk of maritime activities. There is no archaeological evidence of this *opus pilarum* structure, but the anchorage contexts for harbour activity are grouped in this waterfront, predominantly for the Punic and Roman periods. These finds, however, confirm that anchoring activity took place here.

Based on these data, it seems likely that there was an artificial structure that fulfilled the role of a breakwater and explains the large amount of anchoring material in an area where this does not appear to be the safest of activities. This structure could well correspond to the *opus pilarum* to which the inscription refers, or another type of structure still undocumented by archaeology that could have been located somewhere in the southeast corner of the ancient city. A structure like this would prevent wave height above 0.6 m in 46% of the scenarios with different wind direction and intensity included.

Conclusion

This study offers for the first time a quantifiable image of the effect of waves on the interior of an ancient harbour, such as that of ancient Carthago Nova. Combining data from geoarchaeology, underwater archaeology and applying oceanography techniques has allowed us to reconstruct the maritime landscape and to better understand the dynamics of harbour traffic in Antiquity.

Mobility over time in the use of anchoring areas has been proved in the case of ancient Carthago Nova. At first (third century BC), the anchoring was carried out in the safest area of the Mandarache. Subsequently (fourth century AD), this activity was moving towards the Espalmador, far from the waterfront of the city. The impact and evolution of wind waves can be found as one of the causes of this mobility. Vessels were looking for the safest spaces for anchoring.

The results of the SWAN model in ancient Carthago Nova in relation to archaeological data show possible anchoring areas (ASI analysis). On the other hand, in some areas where anchoring was riskier, archaeological anchorage sites have been revealed. Possible modifications of the harbour infrastructure to overcome the effect of the waves can be suggested for the first century BC, possibly with the construction of a breakwater that was built over or modified in the Neronian period.

Results from this new methodology suggest that it can be applied on a larger-scale re-analysis of the use of the spaces inside the ancient Mediterranean harbours. Other works carried out on a large scale (Safadi 2016) and small-scale, like the ones in Portus (Millet et al. 2014), Alexandria, Tyre (Marriner et al. 2008) or Marseille (Millet et al. 2000) lead to this conclusion. The analysis of Carthago Nova is further strengthened by the incorporation of findings from underwater archaeological surveys and a nautical and maritime interpretation of the wave hindcasting results, where the ASI analysis has proved to be a true new methodology. Ancient anchorage harbour areas, slipways, shipyards, quays or breakwaters can be analysed from a different perspective now, in order to understand the effect of synoptic conditions for anchoring and navigation. As a result of this study, it is possible to look at the ancient harbours from their conception for their nautical usefulness.

Finally, the classical literary sources offer a great deal of valuable information that taken together with analysis of archaeological, geomorphological data, and numerical simulation methods, such as those presented here, will undoubtedly improve our understanding of such places in detail. In this study, it has been proved that wave behaviour in the harbour of ancient Carthago Nova with its peculiar topography gave it its unique natural anchoring conditions. As Silius Italicus says, *impensio naturae adiuta fauore* (“blessed with the great good will of Nature” 15.220). Even in modern times, the admiral Andrea Doria used to say that the most secure harbour in the Mediterranean was “[that] of Cartagena and June and July” (Braudel 1995: 1. 257).

Acknowledgements This article is part of the *Carthago Nova: surveying and planning of a privileged Mediterranean city I and II* Project, funded by the General Department of Research of the Ministry of Science and Technology of Spain and by FEDER grants (HAR2011-29330, HAR2014-57672-P and HAR2017-85726-C2-1-P). We thank Puertos del Estado for providing the oceanic data used in the modelling. We would also like to thank the reviewers and editor for their recommendations and comments that have helped improve this paper.

Funding This study was supported by General Department of Research of the Ministry of Science and Technology of Spain and by FEDER grants (HAR2011-29330, HAR2014-57672-P and HAR2017-85726-C2-1-P).

Compliance with Ethical Standards

Conflict of interest The authors declare that they have no conflict of interest directly or indirectly connected to this research.

Human and Animal Rights The research complies with ethical standards and does not involve human participants or animals.

References

- Abascal Palazón JM, Ramallo Asensio SF (1997) La Ciudad de Carthago Nova: La documentación epigráfica. EDITUM
- Arellano Gañán I, Gómez Bravo M, Miñano Domínguez A, Pinedo Reyes, J. (1997) Informe preliminar del corte estratigráfico de El Espalmador Grande (Puerto de Cartagena). *Memorias de Arqueología* 6:303–309, Murcia
- Arnaud P (2005) Les routes de la navigation antique: Itinéraires en Méditerranée. Éditions Errance
- Barr C, Tibby J, Leng MJ, Tyler JJ, Henderson ACG, Overpeck JT, Simpson GL, Cole JE, Phipps SJ, Marshall JC, McGregor GB, Hua Q, McRobie FH (2019) Holocene El Niño-Southern Oscillation variability reflected in subtropical Australian precipitation. *Sci Rep* 9:1627
- Barua DK (2017) Seabed roughness of coastal waters. In: Makowski C, Finkl C (eds) *Encyclopedia of coastal science*. Encyclopedia of earth sciences series. Springer, Cham
- Beresford J (2013) The ancient sailing season. Brill, Leiden- Boston
- Blaauw M (2010) Methods and code for ‘classical’ age-modelling of radiocarbon sequences. *Quat Geochronol* 5:512–518. <https://doi.org/10.1016/j.quageo.2010.01.002>
- Boetto G (2010) Le port vu de la mer: l’apport de l’archéologie navale à l’étude des ports antiques. *Bolletino di Archeologia Online Special issue: XVII International Congress of Classical Archaeology, Roma 22–26 September 2008*
- Booij N, Ris RC, Holthuijsen LH (1999) A third-generation wave model for coastal regions: 1. Model description and validation. *JGR Oceans* 104:7649–7666. <https://doi.org/10.1029/98JC02622>
- Braudel F (1995) The mediterranean and the mediterranean world in the age of Philip II. 2 vols. Berkeley: University of California Press
- Calmel-Avila M (2014) The LIA in Guadalestín valley (Murcia, SE Spain). *Mediterranean* 122:113–119
- Carretero JC, Alvarez E, Gomez M, Perez B, Rodríguez I (2000) Ocean forecasting in narrow shelf seas: application to the Spanish coasts. *Coast Eng* 41:269–293
- Cavaleri L (2005) The wind and wave atlas of the Mediterranean Sea—the calibration phase. *Adv Geosci Eur Geosci Union* 2:255–257
- Cavaleri L, Bertotti L, Lionello P (1991) Wind wave cast in the Mediterranean Sea. *JGR Oceans* 98(C8):10739–10764. <https://doi.org/10.1029/91JC00322>
- Cerezo-Andreo F (2016) Los puertos antiguos de Cartagena: geoarqueología, arqueología portuaria y paisaje marítimo: un estudio desde la arqueología náutica. Ph.D. Dissertation Universidad de Murcia. <http://hdl.handle.net/10201/51041>
- Cerezo-Andreo F (2017) Los puertos antiguos de Carthago Nova, nuevos datos desde la arqueología marítima y geoarqueología portuaria. In: Campos Carrasco J, Bermejo-Meléndez J (eds) *Los puertos atlánticos béticos y lusitanos y su relación comercial con el Mediterráneo*. Hispania Antigua, Serie Arqueologica, vol 7, pp 435–475
- Cibecchini F (2008) Tonnellagi e rotte in età repubblicana: Il contributo dei relitti del Mediterraneo Occidentale. In: Pérez J, Berlanga G (eds) *V Jornadas de Arqueología Subacuática*, pp 483–499
- Conde Guerri E (2003) La ciudad de Carthago Nova: la documentación literaria: (inicios-julioclaudios). EDITUM, Murcia
- Davis RE, Hayden BP, Gay DA, Phillips WL, Jones GV (1997) The North Atlantic Subtropical Cyclone. *J Clim* 10:728–744
- de Juan Fuertes C (2013) Los veleros de comercio romano del Mediterráneo Occidental: análisis de familias y firmas arquitecturales (s. III a.C.—II d.C.). Ph.d. Thesis. University of Valencia
- ECMWF (2017) <https://www.ecmwf.int>
- Fernández Matallana F (2008) Prospección subacuática en la Marina de Curra (Cartagena). In: Lechuga M, Collado PE (eds) *XIX Jornadas de Patrimonio Cultural de la Región de Murcia*, pp 381–383

- Fernández-Montblanc T, Izquierdo A, Bethencourt M (2018) Scattered shipwreck site prospection: the combined use of numerical modelling and documentary research (Fougueux, 1805). *Archaeol Anthropol Sci* 10:141–156. <https://doi.org/10.1007/s12520-016-0348-6>
- Ford B (2011) *The archaeology of maritime landscapes*. Springer, Berlin
- Giaime M, Morhange C, Cau Ontiveros MA, Fornós JJ, Vacchi M, Marriner N (2017) In search of Pollentia's southern harbour: geoarchaeological evidence from the Bay of Alcúdia (Mallorca, Spain). *Palaeogeogr Palaeoclimatol Palaeoecol* 466:184–201. <https://doi.org/10.1016/j.palaeo.2016.11.023>
- Gómez Lahoz M, Carretero Albiach JC (2005) Wave forecasting at the Spanish coast. *J Atmos Ocean Sci* 10(4):389–405
- González Ponce FJ (1995) *Avieno y el Periplo*. Gráficas Sol, Ecija
- Guillaume A, Lefevre JM, Mognard NM (1992) The use of altimeter data to study wind and wave variability in the mediterranean-sea and validate fine-mesh meteorological models. *Oceanol Acta* 15(5):555–561
- Guillermo Marínez M (2014) *Cartagena Medieval*. Cuadernos monográficos, Fundación Teatro Romano de Cartagena, Cartagena
- Hasselmann K et al (1973) Measurements of wind-wave growth and swell decay during the Joint North Sea Wave Project (JONSWAP). *Deutsche Hydrographische Zeitschrift, Reihe*, No.12
- Heburn GW, La Violette PE (1990) Variations in the structure of the anticyclonic gyres found in the Alboran Sea. *JGR Oceans* 95(C2):1599–1613
- Houmb OG, Overvik T (1976) Parametrization of wave spectra and long term joint distribution of wave height and period. In: *Proceedings, first international conference on behaviour of offshore structures (BOSS)*, Trondheim, pp 144–169
- Holthuijsen LH, Booij N, Ris RC, Haagsma IJG, Kieftenburg AT, Kriebitz, EE, Zijlema, M, van der Westhuysen AJ (2004) *SWAN Cycle III Version 40.31 User Manual*. Delft University of Technology, the Netherlands
- Kaniewski D, Marriner N, Morhange C, Faivre S, Otto T, Campo EV (2016) Solar pacing of storm surges, coastal flooding and agricultural losses in the Central Mediterranean. *Sci Rep* 6:25197 (2016). <https://doi.org/10.1038/srep25197>
- Komen GJ, Cavaleri L, Donelan M, Hasselmann K, Hasselmann S, Janssen PA (1994) *Dynamics and modelling of ocean waves*. Cambridge University Press, Cambridge
- La Violette PE (1990) The western Mediterranean circulation experiment (WMCE): introduction. *LGR Oceans* 95:1511–1514
- Lillo Carpio MJ, Rodríguez Estrella T (1996) Aspectos sobre la geomorfología del valle y ensenada de Escambreras (Murcia). *Papeles de Geografía* 23–24:193–210
- Liste M, Méndez FJ, Losada IJ, Medina R, Olabarrieta M (2004) Variaciones Hiperanuales de parámetros medios de Oleaje en el litoral Mediterráneo Español en los últimos cincuenta años: efectos sobre la costa. In: García Codron JC, Diego Liaño C (eds) *El Clima entre el Mar y la Montaña*. Asociación Española de Climatología y Universidad de Cantabria, Santander, pp 51–62
- Ljungqvist FC (2010) A new reconstruction of temperature variability in the extra-tropical northern hemisphere during the last two millennia. *Geogr Ann Ser Phys Geogr* 92:339–351. <https://doi.org/10.1111/j.1468-0459.2010.00399.x>
- Manteca JI, Ros-Sala M, Ramallo-Asensio SF, Navarro-Hervás F, Rodríguez-Estrella T, Cerezo-Andreo F, Ortiz-Menéndez JE, de-Torres T, Martínez-Andreu M (2017) Early metal pollution in southwestern Europe: the former littoral lagoon of El Almarjal (Cartagena mining district, S.E. Spain). A sedimentary archive more than 8000 years old. *Environ Sci Pollut Res* 24(11):10584–10603. <https://doi.org/10.1007/s11356-017-8682-5>
- Marriner N, Goiran JP, Morhange C (2008) Alexander the Great's tombs at Tyre and Alexandria, eastern Mediterranean. *Geomorphology* 100:377–400. <https://doi.org/10.1016/j.geomorph.2008.01.013>
- Mas J (2005) El puerto de Cartagena y su hinterland en la vanguardia de la arqueología submarina española. *Scombraria: La Historia Oculta Bajo El Mar*. Museo Arqueológico de Murcia, Murcia, pp 48–65
- McDermott F, Matthey D, Hawkesworth C (2001) Centennial-scale Holocene climate variability revealed by a high-resolution speleothem $\delta^{18}\text{O}$ record from SW Ireland. *Science* 294:1328–1331
- Medas S (2004) *De Rebus Nauticis: L'arte della navigazione nel mondo antico* (Studia Archaeologica). L'Erma di Bretschneider, Roma
- Millet B, Blanc F, Morhange C (2000) Modélisation numérique de la circulation des eaux dans le Vieux Port de Marseille vers 600 ans avant J.-C. *Mediterranee* 94:61–64. <https://doi.org/10.3406/medit.2000.3155>
- Millet B, Tronchère H, Goiran J-P (2014) Hydrodynamic modeling of the Roman Harbour of Portus in the Tiber Delta: the impact of the North-Eastern channel on current and sediment dynamics. *Geoarchaeology* 29:357–370. <https://doi.org/10.1002/gea.21485>
- Miñano Domínguez A (2012) Informe del Proyecto de Prospección arqueológica en el Puerto de Cartagena (No. 6), Informes- memoria de las actuaciones de prospección, supervisión e inspecciones técnicas arque-

- ológicas subacuáticas en la Región de Murcia. Museo Nacional de Arqueología Subacuática. ARQUA, Cartagena
- Miñano Domínguez A, Castillo Belinchón R (2014) Últimas campañas arqueológicas subacuáticas del Museo Nacional de Arqueología Subacuática (2011–2012). In: Nieto Prieto X, Bethencourt Núñez M (eds) *Arqueología Subacuática Española: Actas Del I Congreso de Arqueología Náutica Y Subacuática Española*, Cartagena, 14, 15 Y 16 de Marzo de 2013. UCA Editores, Cadiz, pp 221–228
- Moghimi S, Gayer G, Günther H, Shafieefar M (2005) Application of third generation shallow water wave models in a tidal environment. *Ocean Dyn* 55:10–27. <https://doi.org/10.1007/s10236-005-0108-0>
- MOPT (1992) Ministerio de Obras Públicas y Transportes (MOPT). Recomendaciones para Obras Marítimas (ROM 03.91) Oleaje. Anejo I. Clima Marítimo en el Litoral Español. Madrid
- Morhange C, Marriner N, Carayon N (2014) The geoarchaeology of ancient Mediterranean harbours. In: Carcaud N, Arnaud-Fassetta G (eds) *La Géoarchéologie Française Au XXIe Siècle*. CNRS Edition, pp 245–254
- Morton J (1998) *The Role of the Physical Environment in Ancient Greek Seafaring*. Brill
- Ortiz JE, de Torres T, Ramallo-Asensio SF, Ros Sala M (2015) Algoritmos de datación por racemización de aminoácidos de ostrácodos del Holoceno y Pleistoceno superior en la Península Ibérica. *Geogaceta* 58:59–62
- Ostrow SE (1979) The topography of Puteoli and Baiae on the eight glass flasks. In: Puteoli. pp 77–140
- Pinedo Reyes J (1996) Inventario de yacimientos arqueológicos subacuáticos del litoral murciano. *Cuadernos de arqueología marítima* 4:57–90
- Pinedo Reyes J (2012) Actuaciones arqueológicas submarinas en nueva dársena deportiva “Marina de Curra.”. In: *Actas de Las Jornadas de ARQUA 2011 MECD*, Cartagena, pp 47–51
- Pomey P, Tchernia A (1978) Le tonnage maximum des navires de commerce romains. *Archaeonautica* 2:233–251. <https://doi.org/10.3406/nauti.1978.875>
- Poveda P (2015) Méthode de restitution des navires antiques : nouveaux outils et nouvelles analyses des restitutions en archéologie navale. *Revue d'Histoire Maritime* 21:157–179
- Pryor JH (1995) The geographical conditions of galley navigation in the Mediterranean. In: Morrison J (eds), *The age of the galley: Mediterranean Oared vessels since pre-classical times*. London, pp. 206–216
- Puertos del Estado (2017a) Clima medio de oleaje. Boya de Cabo de Palos. Conjunto de Datos: Red Exterior. Código B.D.2610. Banco de Datos oceanográficos de Puertos del Estado
- Puertos del Estado (2017b) Clima medio de viento. Estacion de Cartagena-Escombreras. Conjunto de Datos: REMPOR. Código B.D.4621. Banco de Datos oceanográficos de Puertos del Estado. http://calipso.puertos.es/BD/informes/medios/MED_3_4_4621.pdf
- Puertos del Estado (2017c) Punto SIMAR 0.98 °W, 37.58 °N Código 611037012. <http://www.puertos.es/es-oceanografia/Paginas/portus.aspx>
- Ramallo Asensio SF, Martínez Andreu M (2010a) El puerto de Carthago Nova: Eje de vertebración de la actividad comercial en el sureste de la Península Ibérica. *Bolletino di Archeologia Online, Bollettino di Archeologia on line Special issue*, pp 141–159
- Ramallo Asensio SF, Murcia Muñoz AJ (2010) Aqua et lacus in Carthago Nova. *Zeitschrift für Papyrologie und Epigraphik* 172:249–258
- Ramallo Asensio SF, Ros Sala M, Cerezo-Andreo F, Manteca JI, Rodríguez Estrella T, Navarro Hervas F, Martínez Andreu M, Torres T, Ortiz JE, García León J, Fernández Díaz A (2016) Carthago Nova: Topografía y urbanística de una urbe mediterránea privilegiada. El Proyecto Arqueotopos, in: IKUWA V—Congreso Internacional de Arqueología Subacuática, Cartagena, pp 513–528
- Rodrigo FS (2018) A review of the little ice age in Andalusia (Southern Spain): results and research challenges. *Geogr Res Lett* 44(1):245–265
- Safadi C (2016) Wind and wave modelling for the evaluation of the maritime accessibility and protection afforded by ancient harbours. *J Archaeol Sci Rep* 5:348–360. <https://doi.org/10.1016/j.jasrep.2015.12.004>
- Salomon F, Keay S, Carayon N, Goiran JP (2016) The development and characteristics of ancient harbours—applying the PADM chart to the case studies of Ostia and Portus. *PLoS One* 11:e0162587. <https://doi.org/10.1371/journal.pone.0162587>
- Sánchez-Arcilla A, González-Marco D, Bolaños R (2008) A review of wave climate and prediction along the Spanish Mediterranean coast. *Nat Hazards Earth Syst Sci* 8:1217–1228
- Sánchez-López G, Hernández A, Pla-Rabes S, Trigo RM, Toro M, Granados I, Sáez A, Masqué P, Pueyo JJ, Rubio-Inglés MJ, Giral S (2016) Climate reconstruction for the last two millennia in central Iberia: the role of East Atlantic (EA), North Atlantic Oscillation (NAO) and their interplay over the Iberian Peninsula. *Quat Sci Rev* 149:135–150. <https://doi.org/10.1016/j.quascirev.2016.07.021>

- Seisdedos J, Mulas J, González de Vallejo LI, Rodríguez Franco JA, Gracia FJ, del Río L, Garrote Revilla J (2013) Estudio y cartografía de los peligros naturales costeros de la región de Murcia. *Boletín geológico y minero* 124:505–520
- Stefanakos ChN, Athanassoulis GA, Cavaleri L, Bertotti L, Lefèvre JM (2004)a. Wind and Wave Climatology of the Mediterranean Sea. Part I: Wind Statistics. In: Proceedings of the fourteenth International Offshore and Polar Engineering Conference. Toulon, pp 117–186
- Stefanakos ChN, Athanassoulis GA, Cavaleri L, Bertotti L, Lefèvre JM (2004)b. Wind and Wave Climatology of the Mediterranean Sea. Part II: Wave Statistics. In: Proceedings of the fourteenth international offshore and polar engineering conference. Toulon, pp 187–196
- Stock F, Pint A, Horejs B, Ladstätter S, Brückner H (2013) In search of the harbours: new evidence of Late Roman and Byzantine harbours of Ephesus. *Quatern Int* 312:57–69. <https://doi.org/10.1016/j.quaint.2013.03.002>
- Strachan-Davidson JL (1888) *Selections from Polybius*. Clarendon Press, Oxford
- Tofiño de San Miguel V (1787) *Derrotero de las costas de España en el Mediterraneo: y su correspondiente de Africa para inteligencia y uso de las cartas esféricas presentadas al rey nuestro señor*. Vda. de Ibarra e Hijos, Madrid
- Torres T, Ramallo Asensio SF, Sánchez-Palencia Y, Ros Sala M, Ortiz JE, Navarro F, Cerezo-Andreo F, Rodríguez-Estrella T, Manteca I (2018) Reconstructing human–landscape interactions in the ancient Mediterranean harbour of Cartagena (Spain). *Holocene* 28(6):879–894. <https://doi.org/10.1177/0959683617752838>
- Viúdez A, Tintoré J, Haney RL (1996a) Circulation in the alboran sea as determined by quasi-synoptic hydrographic observations. Part I: three-dimensional structure of the two anticyclonic gyres. *J Phys Oceanogr* 26:684–705
- Viúdez A, Tintoré J, Haney RL (1996b) Circulation in the Alboran Sea as determined by quasi-synoptic hydrographic observations. Part II: Mesoscale ageostrophic motion diagnosed through density dynamical assimilation. *J Phys Oceanogr* 26:706–724
- WAM-DI Group (1988) The WAM model—a third generation ocean wave prediction model. *J Phys Oceanogr* 18:1775–1810
- Westerdahl C (2011) The maritime cultural landscape. In: Ford B, Catsambis A, Hamilton DL (Eds) *The Oxford handbook of maritime archaeology*, pp 733–763
- Wolf J, Hargreaves JC, Flather RA (2000) Application of the SWAN shallow water wave model to some UK coastal sites, Proudman Oceanographic Laboratory Report
- WRC (2004) *Wind and wave atlas of the mediterranean sea*. Western European Armaments Organisation Research Cell

Publisher's Note Springer Nature remains neutral with regard to jurisdictional claims in published maps and institutional affiliations.